Proceedings of the Thirty-Fifth International Joint Conference on Artificial Intelligence (IJCAI-26)
Special Track on AI and Social Good

When Can We Trust Fairness Audits? Identifying Reliability Boundaries of Third-party Audit Conclusions

Yuanhao Liu[1,2], **Qi Cao**[1,*] and **Huawei Shen**[1]

[1]State Key Laboratory of AI Safety, Institute of Computing Technology, Chinese Academy of Sciences
[2]University of Chinese Academy of Sciences
{liuyuanhao20z, caoqi, shenhuawei}@ict.ac.cn

Abstract

Fairness auditing aims to assess whether a model is fair, playing a critical role in identifying potential risks in deployed AI systems. In practice, due to limited access, third-party auditors often rely on self-collected datasets (e.g., via sock-puppets), which may differ from real-world deployment scenarios. Such discrepancy can lead to inconsistencies between audit conclusions on the collected data and those in actual deployment, raising concerns about the reliability of third-party audits. This motivates a critical question: When can we trust fairness audit conclusions derived from third-party datasets? Answering this question is challenging, as the deployment distribution is typically inaccessible or unobservable. To tackle this, we introduce the *Consistency Radius*, a metric that quantifies the maximum distribution shift under which an audit conclusion based on a third-party dataset remains consistent. We further propose a convex relaxation-based optimization method to estimate the radius using only model responses over the audit dataset. Leveraging this framework, third-party auditors can provide their datasets to model providers and request the distributional discrepancy relative to the deployment distribution, enabling reliable audit conclusions without direct data access.

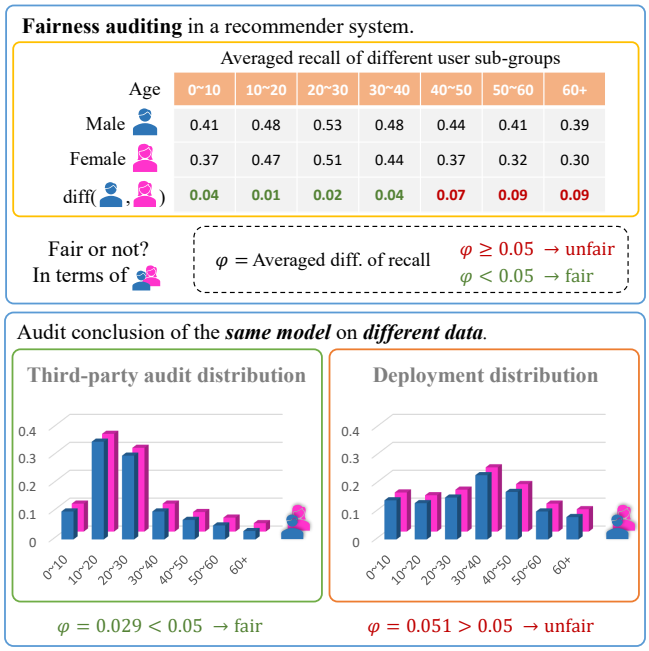

Figure 1: Fairness conclusions are sensitive to distribution shifts. A model showing low disparity on a young-dominated audit distribution may exhibit high disparity on a balanced deployment distribution, reversing the audit conclusion.

1 Introduction

Algorithmic fairness is critical for machine learning systems governing access to opportunities [Chinta *et al.*, 2025; Necula and Păvăloaia, 2023; Shen *et al.*, 2025]. To mitigate systematic discrimination, fairness auditing [Sandvig *et al.*, 2014; Buolamwini and Gebru, 2018], which assesses whether models are fair, has become standard practice for responsible AI.

Fairness auditing generally operates by assessing performance disparities across demographic groups [Bandy, 2021]. Ideally, this assessment would be conducted on the underlying deployment distribution—the "ground truth" population the model actually serves. However, third-party auditors typically lack access to this population due to privacy considerations and commercial barriers [Barlas *et al.*, 2021]. Instead, they rely on *third-party audit datasets* constructed via simulated accounts (sock-puppets) or public benchmarks [Asplund *et al.*, 2020; Kallus *et al.*, 2022]. Inevitably, these third-party datasets suffer from sampling biases and diverge from the unobserved deployment distribution.

This divergence poses a fundamental challenge because fairness metrics are highly sensitive to data distributions [Shao *et al.*, 2024]. Figure 1 illustrates this phenomenon through a fairness audit of a recommender system. Initially, within a young-dominated audit dataset, the model exhibits gender fairness with comparable recommendation accuracy across groups. However, a distribution shift to a balanced population reverses this conclusion to unfair, indicating that audit conclusions derived from a third-party dataset may no

*Corresponding author.

longer hold under the deployment distribution.

In this work, we point out the inconsistency between audit conclusions from third-party data and deployment distribution. Since the actual deployment distribution is unobservable, we cannot directly verify the audit conclusion against it. Instead, we adopt a certification perspective, defining the Consistency Radius as the maximum distribution shift under which an audit conclusion based on a third-party dataset remains consistent. We further propose a convex relaxation-based optimization method to estimate the radius. By definition, the radius serves as a safety margin: the audit conclusion is guaranteed to remain valid as long as the divergence between the audit data and deployment distribution falls within this radius. Practically, the radius allows auditors to verify reliability without accessing private user data by simply comparing the calculated radius against the shift magnitude, which can be provided by model owners.

Collaboration Statement. We collaborated with domain experts from a national technical center for algorithm governance (identity anonymized). They participated in (1) **Problem formulation** of the auditing paradigm with third-party audit data and (2) **Mechanism validation** for our proposed auditing protocol based on the consistency radius.

Evaluation Strategy. Given the inaccessibility of deployment data, we simulate diverse distribution shifts on public datasets to approximate real-world deployment discrepancies. We assess reliability by measuring how often the radius fails to identify shifts that overturn the audit conclusion.

Our contributions are:

- We point out the problem of inconsistency in audits, and define the consistency radius as a metric to reason about auditing consistency to unobserved distributions.
- We propose a convex relaxation-based optimization method to estimate the radius relying solely on model responses over the audit dataset.
- We demonstrate that the consistency radius reliably predicts whether audit conclusions hold under shifts, enabling trustworthy certificates in third-party audits.

2 Related Works

Empirical Fairness Auditing. Fairness auditing is a primary mechanism for evaluating machine learning systems in high-stakes domains [Raji *et al.*, 2020; Singhal *et al.*, 2025]. In third-party settings, auditors rely on audit datasets from external sampling (e.g., sock-puppets or surveys) [Sweeney, 2013; Trielli and Diakopoulos, 2019; TeBlunthuis *et al.*, 2021]. Despite efforts to improve sampling representativeness [Raji *et al.*, 2020; Imana *et al.*, 2021], a fundamental limitation persists: auditors often lack access to the system's deployment distribution [Barlas *et al.*, 2021; Fabris *et al.*, 2023]. Thus, it is unclear if audit conclusions derived from audit datasets generalize to actual users, rendering empirical audits potentially unreliable under distribution shifts.

Statistical Fairness Guarantees. A few recent works derive statistically reliable fairness conclusions using a limited amount of **unbiased** audit data to infer distribution-level statistics [Taskesen *et al.*, 2021; Maity *et al.*, 2021; Yan and Zhang, 2022; Chugg *et al.*, 2023; Singh *et al.*, 2023; Lo *et al.*, 2025]. While some studies extend these evaluations to shifted distributions [Taskesen *et al.*, 2021], they require access to the target distribution for density ratio estimation. In our strict third-party setting where the deployment distribution is unobservable, these methods are not applicable.

Subgroup Fairness Auditing. Subgroup fairness auditing examines model performance across fine-grained subpopulations, highlighting that coarse-grained metrics can mask severe local disparities [Kearns *et al.*, 2018; Cherian and Candès, 2024; Hsu *et al.*, 2024; Ganta *et al.*, 2024]. These methods aim to identify the subgroups with the poorest fairness, involving a challenging search in multi-dimensional space [Kearns *et al.*, 2019; Cachel and Rundensteiner, 2022]. While related, they differ in scope: subgroup methods evaluate fairness over a predefined set of distribution shifts (corresponding to specific subgroups). In contrast, our method establishes a consistency radius that certifies the reliability of the audit conclusion against any shift within a continuous margin, regardless of the shift form.

3 Problem Formalization

In this section, we begin by formalizing fairness assessment on the audit dataset and then define the consistency radius under distribution shifts.

3.1 Fairness Assessment

Consider a prediction model $f : \mathcal{X} \to \mathcal{Y}$. Each data point $x \in \mathcal{X}$ is associated with a sensitive attribute, which identifies subgroups that should be treated equitably. We focus on binary sensitive attributes, e.g., sex (male/female). While multi-group fairness involves objectives like Max-Min fairness [Martinez *et al.*, 2020; Hashimoto *et al.*, 2018], the binary setting captures the core challenge of auditing consistency under distribution shifts.

We assume access to an audit dataset $D = \{(x_i, y_i)\}_{i=1}^n$ sampled i.i.d. from distribution P. Based on the binary sensitive attribute, D is partitioned into two group-specific subsets, denoted by D_0 and D_1. The fairness of model f is evaluated based on the discrepancy in performance between the two groups [Saleiro *et al.*, 2018; Cachel and Rundensteiner, 2022]. Since the underlying audit distribution P is observed through the dataset D, we estimate its empirical fairness as:

$$\varphi(P) = \frac{1}{|D_0|} \sum_{i \in D_0} m_i - \frac{1}{|D_1|} \sum_{i \in D_1} m_i, \text{where } D \sim P \quad (1)$$

where $m_i = M(f(x_i), y_i)$ is an instance-level performance metric, such as prediction correctness for classification or utility score for recommendation [Li *et al.*, 2021].

Based on this evaluation, a **fairness assessment** is formed as a binary conclusion relative to a tolerance $\epsilon \geq 0$. We formally define the assessment function $\mathcal{A}$ as:

$$\mathcal{A}(f, P, \epsilon) = \begin{cases} \text{fair}, & \text{if } |\varphi(P)| < \epsilon, \\ \text{unfair}, & \text{if } |\varphi(P)| \geq \epsilon. \end{cases}$$

Here, we distinguish between two key terms: *fairness evaluation* refers to the numerical value $\varphi(P)$, while *fairness assessment* refers to the logical conclusion $\mathcal{A}(f, P, \epsilon)$.

3.2 Consistency Radius

A fundamental challenge in fairness auditing is the potential discrepancy between the audit distribution P, from which the dataset D is sampled, and the target distribution P_h where the model is deployed. Since P_h is often unknown, we aim to measure the robustness of the fairness assessment against potential shifts from P to P_h.

We characterize the shift from P to P_h using a density ratio function $h : \mathcal{X} \times \mathcal{Y} \to \mathbb{R}_+$, so that the target distribution can be viewed as a reweighted version of the audit distribution P:

$$\begin{aligned} P_h(x, y) &= h(x, y) \cdot P(x, y), \\ \text{s.t.} \mathbb{E}_{(x,y)\sim P}[h(x, y)] &= 1. \end{aligned} \tag{2}$$

By introducing the empirical likelihood assumption [Owen, 2001], we approximate this population shift by assigning a discrete weight h_i to each observed sample $(x_i, y_i) \in D$. The vector $\mathbf{h} = [h_1, \ldots, h_n]^\top$ represents the discrete density ratio, subject to $\frac{1}{n}\sum_{i=1}^{n} h_i = 1$. This formulation models distribution shifts solely by altering the probability mass assigned to each data point in $\mathcal{X} \times \mathcal{Y}$, while the intrinsic relation of features, labels, and sensitive attributes remains invariant.

Under a hypothesized shift $\mathbf{h}$, the fairness evaluation on the shifted distribution P_h becomes a weighted average:

$$\varphi(P_h) = \frac{\sum_{i\in D_0} h_i m_i}{\sum_{i\in D_0} h_i} - \frac{\sum_{i\in D_1} h_i m_i}{\sum_{i\in D_1} h_i}. \tag{3}$$

We similarly define the assessment on the shifted distribution P_h as $\mathcal{A}(f, P_h, \epsilon) =$ fair if $|\varphi(P_h)| < \epsilon$, and unfair otherwise.

We define the consistency radius $R(f, P, \epsilon)$ as the maximum magnitude of distribution shift that the fairness assessment can withstand.

Definition 1 (Consistency Radius)**.** *Given a model f, an audit distribution P, and a threshold ϵ, the consistency radius is:*

$$R(f, P, \epsilon) := \sup\left\{ r \geq 0 \;\middle|\; \begin{aligned} d(\mathbf{h}) \leq r \Rightarrow\ & \mathcal{A}(f, P_h, \epsilon) \\ & = \mathcal{A}(f, P, \epsilon). \end{aligned} \right\},$$

where $d(\mathbf{h})$ is a measurement of divergence between distributions after and before a shift $\mathbf{h}$. □

The definition is agnostic to the divergence measure; unless otherwise specified, we adopt the discrete Kullback–Leibler (KL) divergence as d, i.e., $d(\mathbf{h}) = KL(P_h||P) = \frac{1}{n}\sum_{i=1}^{n} h_i \log h_i$.

Intuitively, the consistency radius R serves as a "safety margin" for the audit conclusion. Based on Pinsker's inequality [Csiszár and Körner, 2011], a larger R guarantees that the fairness assessment remains valid for any shift within the KL radius, which allows the probability of any event in the deployment environment to deviate from the audit environment by up to $\sqrt{R/2}$.

4 Methodology

In this section, we model the computation of the consistency radius as a constrained optimization problem and propose a convex-based optimization algorithm to estimate the consistency radius of fairness assessment.

Supplementary material including code and additional details is available at: https://unitdan.github.io/#consistency-radius.

4.1 Convex Relaxation for Optimization

To facilitate optimization, we vectorize the fairness evaluation $\varphi(P_h)$ in Equation 3. With n denoting the sample size of the audit dataset, we define the performance vector $\mathbf{m} \in \mathbb{R}^n$ where $m_i = M(f(x_i), y_i)$, and the group indicator vector $\mathbf{g} \in \{0, 1\}^n$. Equation 3 is rewritten as:

$$\varphi(P_h) = \frac{((1-\mathbf{g}) \odot \mathbf{m})^\top \mathbf{h}}{(1-\mathbf{g})^\top \mathbf{h}} - \frac{(\mathbf{g} \odot \mathbf{m})^\top \mathbf{h}}{\mathbf{g}^\top \mathbf{h}}, \tag{4}$$

where $\odot$ is the Hadamard product. The terms $(1-\mathbf{g})^\top \mathbf{h} = \sum_{i\in D_0} h_i$ and $\mathbf{g}^\top \mathbf{h} = \sum_{i\in D_1} h_i$ represent the effective sample mass of the two groups, respectively.

We formulate the computation of the consistency radius $R(f, P, \epsilon)$ as a constrained optimization problem:

$$\begin{aligned} R(f, P, \epsilon) \quad &= \min_{\mathbf{h}} d(\mathbf{h}), \\ \text{s.t.} \quad & \mathbf{h} \in \mathcal{H} \text{ and } \mathcal{A}(f, P_h, \epsilon) \neq \mathcal{A}(f, P, \epsilon). \end{aligned} \tag{5}$$

Here, $\mathcal{H} := \{h \in \mathbb{R}_+^n : \mathbf{1}^\top \mathbf{h} = n\}$ ensures the validity of the density ratio, while the constraint of $\mathcal{A}(f, P_h, \epsilon) \neq \mathcal{A}(f, P, \epsilon)$ indicates $|\varphi(P_h)| < \epsilon$ if $|\varphi(P)| \geq \epsilon$ and $|\varphi(P_h)| \geq \epsilon$ if $|\varphi(P)| < \epsilon$.

The objective $d(\mathbf{h})$ (KL divergence) is strictly convex. However, the feasible region of the fairness constraint is non-convex. Direct application of greedy methods (e.g., an interpolation by the direction of the gradient of $|\varphi(P_h)|$) to Equation 5 is prone to getting stuck in local optima due to this non-convexity. In the context of safety auditing, such local optima are dangerous as they lead to an overestimation of the audit's consistency (i.e., failing to discover the true minimal shift required to break fairness).

To avoid local optimality, we adopt a convex relaxation approach. We replace the non-convex fairness measurement $|\varphi(P_h)|$ with a linear surrogate $\mathbf{w}^\top \mathbf{h}$, justified by the *Proxy-band Concentration* proposition:

Proposition 1 (Proxy-band Concentration)**.** *Let $H_\phi := \{\mathbf{h} \in \mathcal{H} : \varphi(P_h) = \phi\}$ be the set of $\mathbf{h}$ with the same level of fairness. For two points $\mathbf{h}, \mathbf{h}'$ sampled from H_ϕ and any vector $\mathbf{w} \in \mathbb{R}^n$, for any $\beta \in (0, 1)$, the following concentration bound holds:*

$$P\big(|\mathbf{w}^\top \mathbf{h} - \mathbf{w}^\top \mathbf{h}'| \leq \frac{A \cdot B}{\beta}\big) \geq 1 - \beta, \tag{6}$$

where $A = \sqrt{\mathbb{E}[\|\mathbf{h} - \mathbf{h}'\|^2]}$, and B quantifies the misalignment between $\mathbf{w}$ and the gradient of φ:

$$B = \sqrt{\mathbb{E}_{\mathbf{h},\mathbf{h}'\in H_\phi}\left[\left(\int_0^1 \|\mathbf{w} - \nabla\varphi(\mathbf{h}' + t(\mathbf{h} - \mathbf{h}'))\|\, dt\right)^2\right]}.$$

This proposition can be proved by applying a line-integral decomposition to $\varphi(P_h) - \varphi(P_{h'}) = 0$ for $\mathbf{h}, \mathbf{h}' \in H_\phi$.

Equation 6 indicates that the bandwidth AB/β is controlled by the effective diameter A of the H_ϕ and the gradient-misalignment term B. Since A is determined by the geometry of H_ϕ and is not controllable, we can minimize the bandwidth by reducing B, which requires $\mathbf{w}$ to align closely with $\nabla\varphi$ over H_ϕ. Consequently, a narrower band means that any distribution shifts $\mathbf{h}$ and $\mathbf{h}'$ with the same fairness value $\varphi(P_h) = \varphi(P_{h'})$ will also have nearly identical linear proxy values, i.e., $\mathbf{w}^\top \mathbf{h} \approx \mathbf{w}^\top \mathbf{h}'$.

4.2 Linearizing the Fairness Constraint

According to Proposition 1, minimizing the proxy-band width requires the surrogate vector $\mathbf{w}$ to align with the gradient $\nabla\varphi(P_h)$ on the constraint set H_ϕ. To characterize this ideal direction, we differentiate Equation 4 and obtain:

$$\nabla\varphi(P_h)_i = \underbrace{\frac{(-1)^{g_i}}{N_{g_i}(\mathbf{h})}}_{\text{Scale Term}} \cdot \underbrace{(m_i - \mu_{g_i}(\mathbf{h}))}_{\text{Deviation Term}}, \tag{7}$$

where N_{g_i} and μ_{g_i} denote the total mass and weighted mean of the group containing sample i:

$$N_{g_i}(\mathbf{h}) = \sum_{j \in G_{g_i}} h_j, \quad \mu_{g_i}(\mathbf{h}) = \frac{1}{N_{g_i}(\mathbf{h})} \sum_{j \in G_{g_i}} h_j m_j.$$

In principle, the optimal $\mathbf{w}$ varies across different sets H_ϕ. Since both $N_{g_i}(\mathbf{h})$ and $\mu_{g_i}(\mathbf{h})$ depend on the unknown distribution shift $\mathbf{h}$, directly estimating a separate $\mathbf{w}$ for each H_ϕ is infeasible. We instead construct a static surrogate vector $\mathbf{w}^\star$ by anchoring the approximation at a special H_ϕ with $\phi \approx 0$, where the group-level performances are approximately balanced. This means that the weighted mean $\mu_{g_i}(\mathbf{h})$ of each group is expected to move toward the performance region of the opposing group. Therefore, although the exact value of $\mu_{g_i}(\mathbf{h})$ remains unknown, the opposing group's support range $\mathcal{R}_{\neg i} = [\min_{j \in D_{1-i}} m_j, \max_{j \in D_{1-i}} m_j]$ provides an observable approximation to its plausible location. This allows us to approximate the magnitude of the Deviation Term by measuring how far m_i lies from the opposing group's range.

We therefore define $\mathbf{w}^\star$ as:

$$\mathbf{w}_i^\star = \text{dist}(m_i, \mathcal{R}_{\neg i}) + \delta(m_i), \tag{8}$$

where the function $\text{dist}(x, [a, b]) = \max(0, a - x, x - b)$ measures the distance from m_i to the nearest boundary of $\mathcal{R}_{\neg i}$, and the residual term $\delta(m_i)$ assigns a small positive weight to samples in the overlapping region. In this way, we transform the Deviation Term into a static weight vector $\mathbf{w}^\star$, where each entry measures how far the corresponding sample lies from the anchor condition where $\phi \approx 0$. Intuitively, if $\mathbf{h}$ represents a distribution shift that moves the system toward a fair state, it should place less mass on samples with large $\mathbf{w}_i^\star$, thereby minimizing the linear proxy $\mathbf{w}^{\star\top}\mathbf{h}$. The Scale Term is omitted in this construction and will be incorporated through an optimization regularizer in Section 4.3.

4.3 Consistency Radius Estimation Algorithm

Based on the convex relaxation, we present CoRe (Convex Relaxation for Consistency Radius Estimation). Since $\mathbf{w}^\star$ captures the sample-level sensitivity implied by the fair anchor, the linear proxy $\mathbf{w}^{\star\top}\mathbf{h}$ is expected to be approximately monotonic with the true fairness evaluation. CoRe exploits this monotonicity using a bi-level structure to bridge the numerical gap between the proxy and the true metric:

Inner Level (Convex Optimization). We solve for the optimal distribution shift $\mathbf{h}$ in a convex optimization problem:

$$\begin{aligned} \min_{\mathbf{h}} \quad & d(\mathbf{h}) + \lambda\big((1-\mathbf{g})^\top\mathbf{h} - \mathbf{g}^\top\mathbf{h}\big)^2, \\ \text{s.t.} \quad & \mathbf{w}^{\star\top}\mathbf{h} \le \epsilon_{\text{proxy}} \quad (\text{or } \ge \epsilon_{\text{proxy}}), \text{and } \mathbf{h} \in \mathcal{H}. \end{aligned} \tag{9}$$

Algorithm 1 CoRe: Consistency Radius Estimation

Require: tolerance threshold $\epsilon > 0$, model performance metrics $\mathbf{m} \in \mathbb{R}^n$ and group memberships $\mathbf{g} \in \{0,1\}^n$
Ensure: Consistency Radius R or `infeasible`

```
Compute w* via Eq. 8
Initialize binary search interval [low, high] for ε_proxy
repeat
    ε_proxy ← (low + high)/2
    Solve convex problem (Eq. 9) to obtain h
    if feasible then
        Calculate true fairness evaluation |φ(P_h)|
        if |φ(P_h)| < ε then
            low ← ε_proxy    // Relax proxy constraint
        else
            high ← ε_proxy    // Tighten proxy constraint
        end if
    else
        return infeasible
    end if
until ||φ(P_h)| − ε| < 1 × 10^−5 or max iterations reached
return d(h)
```

Here we incorporate a regularization term $\lambda((1-\mathbf{g})^\top\mathbf{h} - \mathbf{g}^\top\mathbf{h})^2$ to stabilize the Scale Term in Equation 7. Note that the inequality direction ($\le$ or $\ge$) in the condition depends on whether the initial audit is fair or unfair. For brevity, Algorithm 1 illustrates the initially unfair case.

Outer Level (Binary Search). We iteratively calibrate the proxy threshold ϵ_{proxy} via binary search. By tightening or relaxing ϵ_{proxy}, we locate the exact boundary where the resulting true fairness evaluation $|\varphi(P_h)|$ converges to the target tolerance ϵ.

Complexity Analysis. CoRe wraps a convex solver in a binary search loop. Let n denote the size of the audit dataset. The inner strictly convex problem (Eq. 9) is solvable via interior-point methods in $O(n^3)$. In practice, the entropy-based objective typically exhibits faster convergence. With T binary search iterations (typically $T \approx 20$), the total complexity is $O(T \cdot n^3)$, ensuring scalability.

5 Experiments for Evaluating the Method

In this section, we evaluate the proposed estimation method (CoRe). We aim to answer three research questions:

- **RQ1 (Accuracy):** Can the method accurately estimate the consistency radius compared to ground truth and numerical baselines?
- **RQ2 (Effectiveness):** Does the estimated radius serve as a tight and valid lower bound for distributional shifts in complex, real-world scenarios without a ground truth?
- **RQ3 (Stability):** How sensitive is the estimation to the size of the audit dataset?

5.1 Experimental Setup

Datasets. We utilize two synthetic distributions and three real-world datasets covering multiple data types:

Method	ϵ_0	ϵ_1	ϵ_2	ϵ_3	ϵ_4	ϵ_5	ϵ_6	ϵ_7	ϵ_8	ϵ_9	Overall
Greedy-Search	5.25	5.80	6.45	7.12	8.90	10.55	13.20	16.40	19.80	24.15	11.76
Worst-Group	4.87	5.15	6.02	6.63	8.15	9.40	11.85	14.20	17.55	21.30	10.53
CoRe (Ours)	**0.01**	**0.05**	**0.14**	**0.22**	**0.35**	**0.57**	**0.88**	**1.03**	**1.44**	**2.23**	**0.45**

Table 1: Estimation error on the Synthetic Trinomial dataset. The thresholds ϵ_0 to ϵ_9 are ordered by increasing audit margin, where ϵ_0 is closest to the fairness evaluation $\varphi(P)$ and thus represents the most fragile setting. CoRe consistently achieves lower error than the baselines.

- **Synthetic Trinomial:** We constructed a simple dataset from a trinomial distribution $X \in \{0, 1, 2\}$. By grid searching the values of $P(X = i)$, we can discretely traverse all possible distribution shifts to derive a ground-truth consistency radius. We define a sensitive attribute that partitions samples with different values into two groups D_0 (if $X \in \{0, 1\}$) and D_1 (if $X = 2$). Rather than explicitly specifying the model f, label Y, and performance metric function M, we assign a random value m_i to each $X = i$ to simulate the composite model performance metric $M(f(x), y)$ for simplicity. We sample 10 performance vectors and 10 audit distributions, yielding 100 configurations, and test 10 feasible thresholds for each configuration.
- **Synthetic Gaussian:** We constructed a more complex synthetic dataset where $X \sim \mathcal{N}(0, 1)$. Although it is infeasible to traverse all possible distribution shifts to calculate the ground-truth radius for this dataset, we can empirically estimate the consistency radius by constructing specific shifted distributions through simple perturbations (e.g., of the mean and variance). We defined $X \in D_0$ if $X \leq 0$, and D_1 otherwise, to evenly partition the samples into two groups. Similar to the Synthetic Trinomial dataset, we specified the performance metric as $M(x) = \text{sigmoid}(x)$ to avoid explicitly defining the model and labels. The sigmoid function ensures that different samples x yield varying model performance, while also inducing significant performance disparity between the groups D_0 and D_1.
- **Real-World Datasets:** Compared to synthetic datasets, real-world data distributions are significantly more complex. We thus rely on biased sampling to simulate distribution shifts. We employ three widely-used datasets covering structured data, user interaction, and images to demonstrate generalizability:
  - **Adult [Kohavi and others, 1996] (Structured):** Predicting income levels using an MLP classifier.
  - **ML-1m [Harper and Konstan, 2015] (Interaction):** Predicting user preferences in recommendation using LightGCN [He *et al.*, 2020].
  - **CelebA [Liu *et al.*, 2015] (Image):** Predicting the "Smiling" attribute of photos using ResNet-18 [He *et al.*, 2016].

  We set the sensitive attribute as sex (Male/Female) for all the real-world datasets. The performance function M is set to be the prediction correctness for Adult and CelebA, and user-level recall for ML-1m.

For all datasets, we sample n instances (default $n = 1000$) to form the audit set D.

Methods and Baselines. Since no existing baseline directly addresses our problem, we design two comparison methods:

- **Greedy-Search:** A greedy method that searches from the all-ones vector (no distribution shift) along the gradient of $\varphi(P_h)$ to induce the largest fairness changes with the smallest distribution shifts.
- **Worst-Group:** A heuristic strategy inspired by subgroup fairness audits. It identifies the subgroup contributing most to the fairness gap and iteratively adjusts its weight until the fairness threshold is approached.

5.2 RQ1: Accuracy Verification

We evaluate the accuracy of CoRe on the Synthetic Trinomial dataset, where the ground truth radius is explicitly calculable. Specifically, to implement the Worst-Group baseline in this setting, we treat the distinct values within the group D_0 (i.e., $X = 0$ and $X = 1$) as separate subgroups.

Recall that the consistency radius $R(f, P, \epsilon)$ depends on whether the fairness evaluation $\varphi(P)$ falls within the tolerance threshold ϵ. Intuitively, the magnitude of the radius and the difficulty of estimation are influenced by the *audit margin*, which is the difference between the observed evaluation $\varphi(P)$ and the threshold ϵ. Considering this influence, for each audit distribution P, we divide the feasible range of ϵ equally and obtain 10 equally spaced points $\epsilon_0, \ldots, \epsilon_9$, sorted in ascending order of the margin $\big||\varphi(P)| - \epsilon\big|$. Specifically, ϵ_0 denotes minimal margins (which can be fragile and critical), whereas ϵ_9 denotes large margins (requiring large shifts to reverse, thus less critical).

We employ Median Absolute Percentage Error (MdAPE) relative to the ground truth radius as our primary metric to mitigate the influence of extreme outliers.

Table 1 shows error trends across margins. CoRe outperforms baselines on all ϵ settings with a low MdAPE of 0.45. For small margins ($\epsilon_{0\sim4}$), CoRe achieves negligible error (MdAPE < 0.4). This confirms our convex relaxation is tight in critical scenarios. Its larger errors at $\epsilon_{7\sim9}$ mainly stem from the approximation induced by anchoring the surrogate at $\phi \approx 0$. In contrast, Worst-Group yields much higher error because it restricts shifts to a single subgroup axis, while the optimal shift often requires coordinated adjustments over multiple values. Greedy-Search also produces large errors due to entrapment in local optima.

5.3 RQ2: Effectiveness Validation

We next verify if CoRe provides a valid and tight lower bound in a more complex scenario without ground truth. We

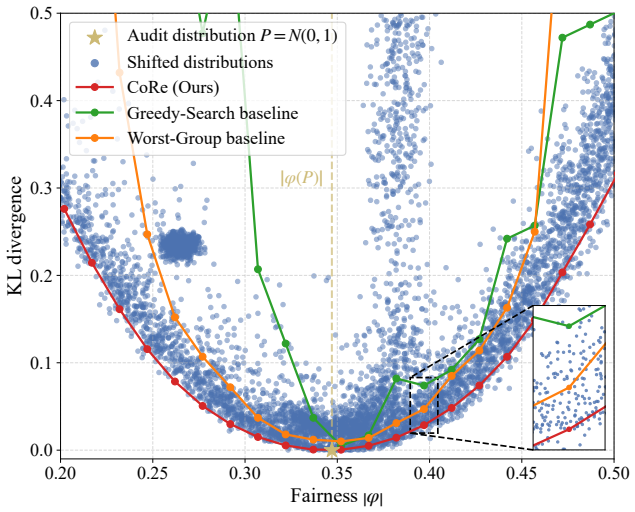

Figure 2: Visual verification on Synthetic Gaussian data. The CoRe curve (Red) tightly hugs the bottom of the scattered distribution shifts, serving as a valid lower bound. In contrast, baseline curves are higher, indicating they overestimate the minimum shift required.

compare CoRe against baselines on the Synthetic Gaussian dataset and the real-world benchmarks. For the Worst-Group, we define subgroups using auxiliary attributes: *sample magnitude* ($|x| < 0.3$, ensuring subgroups have sufficient samples) for the Synthetic Gaussian dataset, *race* (White/Non-White) for Adult and CelebA, and *age* (7 groups) for ML-1m.

We first visually validate the boundary on the Synthetic Gaussian dataset in Figure 2. The audit distribution $\mathcal{N}(0, 1)$ is marked by a star at its fairness evaluation $|\varphi(P)|$. The x-axis represents the fairness metric, and the y-axis represents the distribution shift (KL divergence $d(\mathbf{h})$). The 4,000 scatter points represent parametrically shifted distributions $\mathbf{h}$ at coordinates $(|\varphi(P_h)|, d(\mathbf{h}))$. The curves connect the consistency radii estimated by different methods across a range of auditing thresholds ϵ. Ideally, for any given threshold ϵ, the consistency radius represents the *minimum* shift required to force the fairness evaluation to reach ϵ, forming a tight **lower envelope** along the scatters' bottom edge.

As shown, the CoRe curve (red) tightly hugs the bottom of the scattered points, meaning almost all shifts are bounded. In contrast, the Greedy-Search and Worst-Group curves float significantly higher, leaving many scatter points below them. These points below the curve represent "shortcuts", shifts that overturn fairness with a cost lower than the baselines' estimation, confirming that baselines overestimate the radius and fail to detect the minimal shifts.

For real-world datasets, where we cannot construct parametric shifts, we design an "adversarial" evaluation protocol. Specifically, for a given threshold ϵ, each radius estimation method identifies a critical shifted distribution $\tilde{\mathbf{h}}$ such that the fairness evaluation on $\tilde{\mathbf{h}}$ hits the fairness threshold (i.e., $\varphi(P_{\tilde{h}}) = \epsilon$). To verify the robustness of the estimated radius around this critical point, we generate local adversarial samples by injecting random noise into $\tilde{\mathbf{h}}$. For each $\tilde{\mathbf{h}}$, we generate perturbed distributions $\mathbf{h}'$ by adding random noise of norm α (followed by projection onto the probability simplex to ensure validity).

Dataset	Method	Perturbation Intensity (α)		
		0.01	0.05	0.10
Adult	Greedy-Search	0.44	0.46	0.52
	Worst-Group	0.78	0.86	0.75
	CoRe	**0.02**	**0.01**	**0.00**
ML-1m	Greedy-Search	0.37	0.52	0.67
	Worst-Group	0.60	0.63	0.59
	CoRe	**0.01**	**0.01**	**0.00**
CelebA	Greedy-Search	0.44	0.47	0.62
	Worst-Group	0.83	0.71	0.79
	CoRe	**0.03**	**0.01**	**0.01**

Table 2: Comparison of Local Misjudge Rate (LMR) on real-world datasets. We compare our CoRe against baseline methods across varying perturbation intensities (α).

We compute the Local Misjudge Rate (LMR): the proportion of $\mathbf{h}'$ reversing the conclusion with $d(\mathbf{h}')$ within the radius. High LMR implies a loose radius, failing to exclude risky distributions. We aggregate 100 generated shifts $\mathbf{h}'$ per method for evaluating all methods.

Table 2 reports the LMR across different perturbation intensities ($\alpha \in \{0.01, 0.05, 0.1\}$). **CoRe** consistently maintains the lowest LMR across all noise levels, demonstrating that its estimated boundary is robust even under varying degrees of adversarial perturbation. In contrast, the baselines, particularly Worst-Group, exhibit significantly higher misjudgment rates. This confirms that baselines tend to overestimate the radius, leaving "blind spots" near the boundary that are easily exploited by random perturbations.

5.4 RQ3: Stability with Audit Sample Size

Finally, we examine the sensitivity of CoRe to the size of the audit dataset. This is crucial for practitioners to understand the data requirements for a reliable estimation.

We conduct experiments on the real-world datasets. We vary the audit sample size n from 100 to 2,000. To establish a reference value, we compute the consistency radius using a large sample size ($n = 5,000$). For each setting, we repeat the experiment 20 times to measure the variance arising from sampling randomness.

Figure 3 illustrates the mean estimated radius (solid line) and the standard deviation (shaded region) across different sample sizes. The average estimated radius stabilizes quickly. On all datasets, the estimation converges to the reference value once the sample size reaches approximately $n = 1,000$. The variance of the estimation also decreases significantly as n increases. Even with smaller samples ($n = 500$), the method produces reasonably stable estimates. These results indicate that CoRe is highly data-efficient.

6 Practical Implementation

We present a blind auditing protocol and use simulations to address experts' questions.

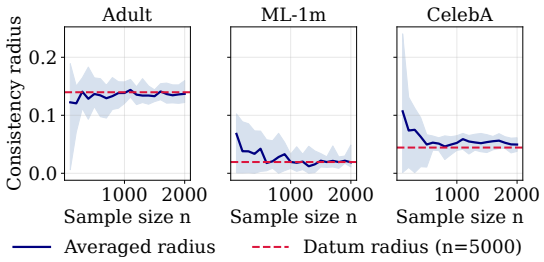

Figure 3: Stability of the estimated radius on real-world datasets as sample size increases. The solid line represents the mean radius over 20 runs, and the shaded area indicates the standard deviation. The estimation converges rapidly, stabilizing around $n = 1,000$.

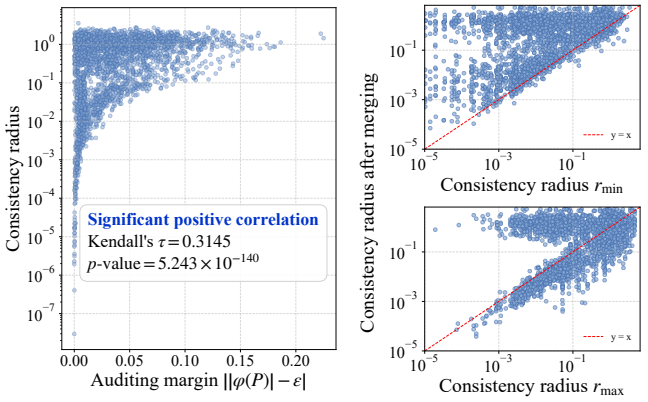

(a) Correlation with Auditing Margin $||\varphi(P)| - \epsilon|$

(b) Merged vs. $r_{\min}$ (upper) and $r_{\max}$ (lower)

Figure 4: **Properties of the Consistency Radius.** (a) There is a significant positive correlation between the radius and the auditing margin. (b) Merging two datasets surpasses the smaller original radius ($r_{\min}$) but not necessarily the larger ($r_{\max}$).

6.1 Consistency Radius in Practice

The consistency radius decouples audit verification from accessing deployment distributions. By determining the consistency radius, the auditors can **verify an audit conclusion solely based on the magnitude of the distribution shift**, which can be requested from the model provider. This property enables a reliable fairness audit that strictly preserves the privacy of the deployment environment.

6.2 The Blind Auditing Protocol

While radius-based verification preserves privacy, self-reported distribution shifts pose a risk of dishonesty. We propose a *Blind Auditing Protocol* to encourage honest reporting.

In this protocol, auditors present multiple audit datasets and ask model providers to report the magnitude of distribution shift between private deployment data and audit datasets, keeping providers blinded to audit outcomes and radii. This information asymmetry encourages honest reporting but cannot by itself guarantee truthfulness; in practice, it can be complemented by spot checks, contractual penalties, or regulatory oversight. It creates a strategic dilemma: (1) Indiscriminate Denial Risk: Unable to distinguish audit favorability, exaggerating shifts to evade "unfair" verdicts risks invalidating "fair" ones, forfeiting certification; (2) Unknown Escape Boundary: Unaware of the radius, providers cannot determine the minimum falsification to "escape" assessment, rendering manipulation infeasible.

6.3 Addressing Experts' Questions

In the implementation of the protocol, experts raised two questions regarding the properties of the radius. We provide evidence-based answers using synthetic simulations with balanced binary groups and randomly sampled metric values.

Query 1: Can audit margin serve as a safety proxy? The stakeholders inquired whether models with fairness scores further from the threshold ϵ (i.e., a larger audit margin $||\varphi(P)| - \epsilon|$) effectively possess a larger consistency radius against distribution shifts.

Our Response: While the margin does not deterministically quantify the maximum allowable shift (the radius), Figure 4a reveals a significant positive correlation by the Kendall rank test. The concentration of points in the upper-left suggests that a small margin indicates the risk of a small radius.

Expert Takeaway: The margin can be a risk indicator and prioritize precise radius estimation for high-risk evaluations.

Query 2: Does consensus guarantee larger radii? Experts inquired whether multiple audit datasets with the *same* conclusion (e.g., all "fair") can be combined into a more reliable audit dataset with a larger consistency radius.

Our Response: To examine this, we simulated pairwise dataset merging. For each pair of audit datasets that reached the same conclusion, we computed the radius after merging them, denoted by r_{merge}, and compared it with the larger and smaller radii before merging, denoted by $r_{\max}$ and $r_{\min}$, respectively. As shown in Figure 4b, r_{merge} does not consistently exceed $r_{\max}$. Part of the cases lie between $r_{\min}$ and $r_{\max}$, suggesting that consensus in audit conclusions does not necessarily translate into a larger consistency radius.

Expert Takeaway: Consensus may provide useful supporting evidence, but our current analysis does not establish that merging consensus datasets guarantees a larger consistency radius. At this stage, reporting individual radii alongside merged results provides a more transparent practice.

7 Conclusion & Limitations

We addressed fairness fragility under distribution shifts by proposing the Consistency Radius. Our convex relaxation estimator enables blind auditing, bridging static evaluation and dynamic deployment without requiring sensitive user data.

There are also some limitations of our study. First, although we performed rigorous experimental evaluation, due to the inaccessibility of proprietary industrial systems, we could not further validate our method in live production environments. Second, our framework currently focuses on binary sensitive attributes and single fairness conclusions; extending it to intersectional fairness and joint certification of multiple conclusions is left for future work.

Acknowledgments

This work is funded by the Strategic Priority Research Program of the Chinese Academy of Sciences under Grant No. XDB0680201, the National Natural Science Foundation of China under Grant Nos. 62472409, 62272125.

Ethical Statement

There are no ethical issues.

References

[Asplund *et al.*, 2020] Joshua Asplund, Motahhare Eslami, Hari Sundaram, Christian Sandvig, and Karrie Karahalios. Auditing race and gender discrimination in online housing markets. In *Proceedings of the international AAAI conference on web and social media*, volume 14, pages 24–35, 2020.

[Bandy, 2021] Jack Bandy. Problematic machine behavior: A systematic literature review of algorithm audits. *Proceedings of the ACM on Human-Computer Interaction*, 5(CSCW1):1–34, 2021.

[Barlas *et al.*, 2021] Pinar Barlas, Kyriakos Kyriakou, Olivia Guest, Styliani Kleanthous, and Jahna Otterbacher. To "see" is to stereotype: Image tagging algorithms, gender recognition, and the accuracy-fairness trade-off. *Proceedings of the ACM on Human-Computer Interaction*, 4(CSCW3):1–31, 2021.

[Buolamwini and Gebru, 2018] Joy Buolamwini and Timnit Gebru. Gender shades: Intersectional accuracy disparities in commercial gender classification. In *Conference on fairness, accountability and transparency*, pages 77–91. PMLR, 2018.

[Cachel and Rundensteiner, 2022] Kathleen Cachel and Elke Rundensteiner. Fins auditing framework: Group fairness for subset selections. In *Proceedings of the 2022 AAAI/ACM Conference on AI, Ethics, and Society*, pages 144–155, 2022.

[Cherian and Candès, 2024] John J Cherian and Emmanuel J Candès. Statistical inference for fairness auditing. *Journal of machine learning research*, 25(149):1–49, 2024.

[Chinta *et al.*, 2025] Sribala Vidyadhari Chinta, Zichong Wang, Avash Palikhe, Xingyu Zhang, Ayesha Kashif, Monique Antoinette Smith, Jun Liu, and Wenbin Zhang. Ai-driven healthcare: Fairness in ai healthcare: A survey. *PLOS digital health*, 4(5), 2025.

[Chugg *et al.*, 2023] Ben Chugg, Santiago Cortes-Gomez, Bryan Wilder, and Aaditya Ramdas. Auditing fairness by betting. *Advances in Neural Information Processing Systems*, 36:6070–6091, 2023.

[Csiszár and Körner, 2011] Imre Csiszár and János Körner. *Information theory: coding theorems for discrete memoryless systems*. Cambridge University Press, 2011.

[Fabris *et al.*, 2023] Alessandro Fabris, Andrea Esuli, Alejandro Moreo, and Fabrizio Sebastiani. Measuring fairness under unawareness of sensitive attributes: A quantification-based approach. *Journal of Artificial Intelligence Research*, 76:1117–1180, 2023.

[Ganta *et al.*, 2024] Teja Ganta, Arash Kia, Prathamesh Parchure, Min-heng Wang, Melanie Besculides, Madhu Mazumdar, and Cardinale B Smith. Fairness in predicting cancer mortality across racial subgroups. *JAMA Network Open*, 7(7):e2421290–e2421290, 2024.

[Harper and Konstan, 2015] F Maxwell Harper and Joseph A Konstan. The movielens datasets: History and context. *ACM Transactions on Interactive Intelligent Systems (TIIS)*, 5(4):1–19, 2015.

[Hashimoto *et al.*, 2018] Tatsunori Hashimoto, Megha Srivastava, Hongseok Namkoong, and Percy Liang. Fairness without demographics in repeated loss minimization. In *International Conference on Machine Learning*, pages 1929–1938. PMLR, 2018.

[He *et al.*, 2016] Kaiming He, Xiangyu Zhang, Shaoqing Ren, and Jian Sun. Deep residual learning for image recognition. In *Proceedings of the IEEE conference on computer vision and pattern recognition*, pages 770–778, 2016.

[He *et al.*, 2020] Xiangnan He, Kuan Deng, Xiang Wang, Yan Li, Yongdong Zhang, and Meng Wang. Lightgcn: Simplifying and powering graph convolution network for recommendation. In *Proceedings of the 43rd International ACM SIGIR Conference on Research and Development in Information Retrieval*, SIGIR '20, pages 639–648, 2020.

[Hsu *et al.*, 2024] Daniel Hsu, Jizhou Huang, and Brendan Juba. Distribution-specific auditing for subgroup fairness. *arXiv preprint arXiv:2401.16439*, 2024.

[Imana *et al.*, 2021] Basileal Imana, Aleksandra Korolova, and John Heidemann. Auditing for discrimination in algorithms delivering job ads. In *Proceedings of the web conference 2021*, pages 3767–3778, 2021.

[Kallus *et al.*, 2022] Nathan Kallus, Xiaojie Mao, and Angela Zhou. Assessing algorithmic fairness with unobserved protected class using data combination. *Management Science*, 68(3):1959–1981, 2022.

[Kearns *et al.*, 2018] Michael Kearns, Seth Neel, Aaron Roth, and Zhiwei Steven Wu. Preventing fairness gerrymandering: Auditing and learning for subgroup fairness. In *International conference on machine learning*, pages 2564–2572. PMLR, 2018.

[Kearns *et al.*, 2019] Michael Kearns, Seth Neel, Aaron Roth, and Zhiwei Steven Wu. An empirical study of rich subgroup fairness for machine learning. In *Proceedings of the conference on fairness, accountability, and transparency*, pages 100–109, 2019.

[Kohavi and others, 1996] Ron Kohavi et al. Scaling up the accuracy of naive-bayes classifiers: A decision-tree hybrid. In *Kdd*, volume 96, pages 202–207, 1996.

[Li *et al.*, 2021] Yunqi Li, Hanxiong Chen, Zuohui Fu, Yingqiang Ge, and Yongfeng Zhang. User-oriented fairness in recommendation. In *Proceedings of the web conference 2021*, pages 624–632, 2021.

[Liu *et al.*, 2015] Ziwei Liu, Ping Luo, Xiaogang Wang, and Xiaoou Tang. Deep learning face attributes in the wild. In *Proceedings of International Conference on Computer Vision (ICCV)*, December 2015.

[Lo *et al.*, 2025] Victor SY Lo, Sayan Datta, and Youssouf Salami. Bringing practical statistical science to ai and predictive model fairness testing. *AI and Ethics*, 5(3):2149–2164, 2025.

[Maity *et al.*, 2021] Subha Maity, Songkai Xue, Mikhail Yurochkin, and Yuekai Sun. Statistical inference for individual fairness. *arXiv preprint arXiv:2103.16714*, 2021.

[Martinez *et al.*, 2020] Natalia Martinez, Martin Bertran, and Guillermo Sapiro. Minimax pareto fairness: A multi objective perspective. In *International conference on machine learning*, pages 6755–6764. PMLR, 2020.

[Necula and Păvăloaia, 2023] Sabina-Cristiana Necula and Vasile-Daniel Păvăloaia. Ai-driven recommendations: A systematic review of the state of the art in e-commerce. *Applied Sciences*, 13(9):5531, 2023.

[Owen, 2001] Art B Owen. *Empirical likelihood*. Chapman and Hall/CRC, 2001.

[Raji *et al.*, 2020] Inioluwa Deborah Raji, Timnit Gebru, Margaret Mitchell, Joy Buolamwini, Joonseok Lee, and Emily Denton. Saving face: Investigating the ethical concerns of facial recognition auditing. In *Proceedings of the AAAI/ACM Conference on AI, Ethics, and Society*, pages 145–151, 2020.

[Saleiro *et al.*, 2018] Pedro Saleiro, Benedict Kuester, Loren Hinkson, Jesse London, Abby Stevens, Ari Anisfeld, Kit T Rodolfa, and Rayid Ghani. Aequitas: A bias and fairness audit toolkit. *arXiv preprint arXiv:1811.05577*, 2018.

[Sandvig *et al.*, 2014] Christian Sandvig, Kevin Hamilton, Karrie Karahalios, and Cedric Langbort. Auditing algorithms: Research methods for detecting discrimination on internet platforms. *Data and Discrimination: Converting Critical Concerns into Productive Inquiry*, 22(2014):4349–4357, 2014.

[Shao *et al.*, 2024] Minglai Shao, Dong Li, Chen Zhao, Xintao Wu, Yujie Lin, and Qin Tian. Supervised algorithmic fairness in distribution shifts: A survey. *arXiv preprint arXiv:2402.01327*, 2024.

[Shen *et al.*, 2025] Huawei Shen, Yuanhao Liu, Kaike Zhang, Qi Cao, and Xueqi Cheng. The rising safety concerns of deep recommender systems. *The Innovation*, 2025.

[Singh *et al.*, 2023] Harvineet Singh, Fan Xia, Mi-Ok Kim, Romain Pirracchio, Rumi Chunara, and Jean Feng. A brief tutorial on sample size calculations for fairness audits. *arXiv preprint arXiv:2312.04745*, 2023.

[Singhal *et al.*, 2025] Mohit Singhal, Javier Pacheco, Seyyed Mohammad Sadegh Moosavi Khorzooghi, Tanusree Debi, Abolfazl Asudeh, Gautam Das, and Shirin Nilizadeh. Auditing yelp's business ranking and review recommendation through the lens of fairness. In *Proceedings of the International AAAI Conference on Web and Social Media*, volume 19, pages 1798–1816, 2025.

[Sweeney, 2013] Latanya Sweeney. Discrimination in online ad delivery. *Communications of the ACM*, 56(5):44–54, 2013.

[Taskesen *et al.*, 2021] Bahar Taskesen, Jose Blanchet, Daniel Kuhn, and Viet Anh Nguyen. A statistical test for probabilistic fairness. In *Proceedings of the 2021 ACM conference on fairness, accountability, and transparency*, pages 648–665, 2021.

[TeBlunthuis *et al.*, 2021] Nathan TeBlunthuis, Benjamin Mako Hill, and Aaron Halfaker. Effects of algorithmic flagging on fairness: Quasi-experimental evidence from wikipedia. *Proceedings of the ACM on Human-Computer Interaction*, 5(CSCW1), apr 2021.

[Trielli and Diakopoulos, 2019] Daniel Trielli and Nicholas Diakopoulos. Search as news curator: The role of google in shaping attention to news information. In *Proceedings of the 2019 CHI Conference on human factors in computing systems*, pages 1–15, 2019.

[Yan and Zhang, 2022] Tom Yan and Chicheng Zhang. Active fairness auditing. In *International Conference on Machine Learning*, pages 24929–24962. PMLR, 2022.